Aptamer-Targeted Gold Nanoparticles As Molecular-Specific Contrast Agents for Reflectance Imaging

David J. Javier,[†] Nitin Nitin,[†] Matthew Levy,[‡] Andrew Ellington,[‡] and Rebecca Richards-Kortum*[,†]

Department of Bioengineering, Rice University, Houston, Texas 77005, and Institute for Cellular and Molecular Biology, University of Texas at Austin, Austin, Texas 78712. Received March 25, 2008; Revised Manuscript Received April 22, 2008

Targeted metallic nanoparticles have shown potential as a platform for development of molecular-specific contrast agents. Aptamers have recently been demonstrated as ideal candidates for molecular targeting applications. In this study, we investigated the development of aptamer-based gold nanoparticles as contrast agents, using aptamers as targeting agents and gold nanoparticles as imaging agents. We devised a novel conjugation approach using an extended aptamer design where the extension is complementary to an oligonucleotide sequence attached to the surface of the gold nanoparticles. The chemical and optical properties of the aptamer−gold conjugates were characterized using size measurements and oligonucleotide quantitation assays. We demonstrate this conjugation approach to create a contrast agent designed for detection of prostate-specific membrane antigen (PSMA), obtaining reflectance images of PSMA(+) and PSMA(−) cell lines treated with the anti-PSMA aptamer−gold conjugates. This design strategy can easily be modified to incorporate multifunctional agents as part of a multimodal platform for reflectance imaging applications.

I. INTRODUCTION

Most contrast agents for molecular imaging couple a targeting molecule to a reporter moiety. For example, monoclonal antibodies are frequently used as targeting agents coupled to reporting agents. Recently, the use of aptamers for molecular targeting has been advocated due to several advantages relative to traditional antibody-based approaches (*1, 2*). Aptamers are generally smaller in size (3−5 nm) than antibodies (∼12−15 nm). The high affinity and specificity of aptamers make them ideal targeting agents. In contrast to antibodies, aptamers can be chemically synthesized in bulk amounts at a reasonable price. Another advantage of aptamers is that they can be generated using modified nucleotides, and the incorporation of these non-natural analogues can greatly increase nuclease stability. Moreover, oligonucleotide extensions can be easily incorporated in the aptamer's backbone to separate the conjugating arm from the targeting arm. This eliminates the need for direct modifications to the aptamer binding site. In the case of antibodies, the addition of reporting molecules is normally accomplished by modifying functional groups on the peptide backbone which can potentially compromise the affinity of the antibody.

The use of gold nanoparticles as reporting agents for reflectance-based molecular imaging applications has recently been reported as alternative to fluorescence-based methods (*3–5*). Gold nanoparticles have strong localized surface plasmon resonance that makes them ideal for reflectance imaging. The extinction coefficients of gold nanoparticles are higher than organic fluorophores; the scattering signal from a single nanoparticles is approximately equivalent to 10^6 fluorophores in a homogeneous environment (*6, 7*). Gold nanoparticles are good candidates for in vivo applications since their material composition is less cytotoxic compared to organic fluorescent dyes and quantum dots. Moreover, generation of reflectance imaging using gold nanoparticles also requires less complicated instrumentation compared to fluorescence methods.

In a previous study, we demonstrated the development of aptamer-based quantum dot conjugates for molecular imaging where the conjugation of the aptamers to the quantum dot is facilitated using biotin−avidin interactions (*8*). In this paper, we developed aptamer-targeted gold nanoparticles for use as contrast agents for reflectance imaging. In this approach, shown schematically in Figure 1, conjugation of the aptamers to gold nanoparticles is accomplished using an extended aptamer design where the extension is complementary to an oligonucleotide sequence attached to the surface of gold nanoparticles. This novel approach provides a simple conjugation method and offers the potential for multiplexing capabilities.

We demonstrate this conjugation approach to create a contrast agent designed for the detection of prostate-specific membrane antigen (PSMA). PSMA is a cell surface antigen commonly present in prostate cancer cells. Anti-PSMA aptamers were conjugated to 20 nm gold nanoparticles and the optical and chemical properties of the conjugates were characterized. The potential of the conjugates for molecular imaging was demonstrated by obtaining reflectance images of PSMA(+) and PSMA(−) cell lines treated with the anti-PSMA aptamer−gold conjugates.

II. MATERIALS AND METHODS

A. Synthesis of Aptamer−Gold Conjugates. The anti-PSMA aptamer used in the study is an A9 RNA aptamer. The selection and characterization of A9 RNA aptamers have been previously described in another paper (*9*). Here, we added an extension to the aptamer to serve as a hybridization site for complementary oligonucleotide-coated gold nanoparticles. The sequence of the A9 RNA aptamer showing the extended sequence (underlined) is 5′ GGG AGG ACG AUG CGG ACC GAA AAA GAC CUG ACU UCU AUA CUA AGU CUA CGU UCC CAG ACG ACU CGC CCG AGA AUU AAA UGC CCG CCA UGA CCA G. The extended A9 aptamer (100 μM concentration) was obtained from the Ellington laboratory at the University of Texas at Austin.

* E-mail: rkortum@rice.edu.
[†] Rice University.
[‡] University of Texas at Austin.

10.1021/bc8001248 CCC: $40.75
Published on Web 05/31/2008

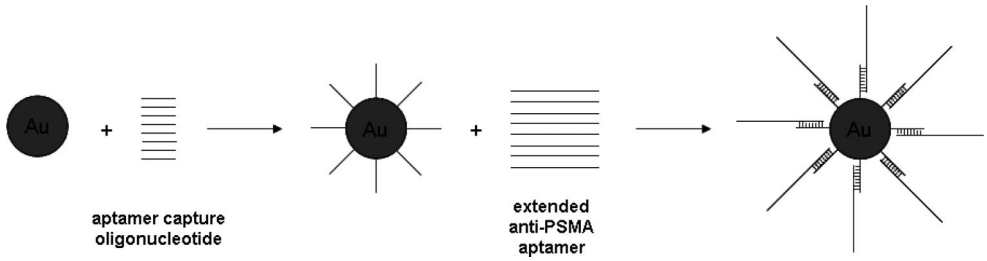

Figure 1. Schematic diagram for the conjugation of anti-PSMA aptamers to gold nanoparticles.

Gold nanoparticles (20 nm gold nanospheres, citrate-stabilized, Ted Pella, Inc.) were coated with capture oligonucleotide which was complementary to the aptamer extension sequence. The aptamer capture oligonucleotide was functionalized with thiol group (C6 S−S spacer) and hexa(ethylene glycol) (18-atom spacer) on the 5′ terminal position. The HPLC-purified aptamer capture oligonucleotide was obtained from IDT DNA Technologies with the following sequence: 5′/ThioMC6-D/Sp18/CTG GTC ATG GCG GGC ATT TAA TTC. To prepare the capture oligonucleotide-coated gold nanoparticles, 5 uM of aptamer capture oligonucleotide was reduced with TCEP (tris(2-carboxyethyl)phosphine hydrochloride, Pierce Chemical) for 30 min and added to 1.0 mL of 20 nm colloidal gold nanoparticles (7.0×10^{11} Au nanoparticles per mL). The conjugate was slowly aged with increasing concentration of PBS for 24 h until a 1× PBS concentration was reached. The unreacted capture oligonucleotide was removed from the oligonucleotide-coated gold nanoparticles by centrifugation (2×) at 12 000 *g* for 30 min. The detailed oligonucleotide coating process is described in a previous paper (*10*).

The anti-PSMA aptamer (50 μL of 100 μM stock solution or 5 nmol) was hybridized to 1.0 mL of capture oligonucleotide-coated gold nanoparticles (suspended in 1× PBS) by initially heating the solution at 70 °C for 5 min followed by incubation at room temperature for 30 min. The unreacted anti-PSMA aptamers were removed from the aptamer−gold conjugates by centrifugation (2×) at 12 000 *g* for 30 min.

B. Characterization of Aptamer−Gold Conjugates. The characterization experiments were designed to determine the size of the conjugates and the amount of aptamer-capture oligonucleotide and the extended anti-PSMA aptamers conjugated to the gold nanoparticles. We used 1.0 mL of 20 nm Au nanoparticles (7.0×10^{11} Au nanoparticles per mL) for all experiments.

The hydrodynamic size of the functionalized gold nanoparticles was measured using dynamic light scattering (Brookhaven Instruments). Triplicate runs were performed at 25 °C and 3 min analysis time to determine the average hydrodynamic diameter of the conjugates.

The amount of aptamer-capture oligonucleotide coated to gold nanoparticles was determined by fluorescence measurements using the Quant-iT OliGreen ssDNA assay kit from Invitrogen. The gold nanoparticles were first dissolved in 500 μM KCN before performing the assay. A standard curve was generated using the aptamer-capture oligonucleotide. The fluorescence intensity ($\lambda_{exc} = 480$ nm, $\lambda_{em} = 520$ nm) of the samples and standards was measured using a plate reader (SpectraMax, Molecular Devices).

The amount of extended anti-PSMA aptamer hybridized to the gold nanoparticles coated with capture oligonucleotides was estimated by using a fluorescently labeled oligonucleotide. Gold nanoparticles coated with capture oligonucleotides were hybridized with a shorter analogue of the anti-PSMA aptamer with a Cy5 modification on the 5′ terminus. The sequence of the oligonucleotide obtained from IDT DNA Technologies is 5′ Cy5\GAA TTA AAT GCC CGC CAT GAC CAG. The oligonucleotide-Cy5 was also used as a standard to generate a calibration curve. The amount of the aptamers hybridized to the gold nanoparticles was estimated by measuring the fluorescence intensity of the oligonucleotide-Cy5 upon dissolution of the gold nanoparticles with KCN and comparing the measured intensity to the standard curve. The solution was treated with KCN to dissolve the gold and release the oligonucleotides, thus preventing the plasmon resonance of gold nanoparticles from interfering with fluorescence measurements.

C. Optical Imaging of Aptamer−Gold Conjugates. LNCaP cells and PC3 prostate cancer cells were obtained from ATCC. LNCaP is used as PSMA(+) cell line, while PC3 served as PSMA(−) cell line. The cells were grown in RPMI media with 5% FBS at 37 °C until they were 80−90% confluent. The cells were trypsinized, washed, and resuspended in 1× PBS before labeling. For cell labeling, the aptamer−gold conjugates (500 μL each) were added to LNCaP and PC3 cell suspensions for 30 min at 37 °C. The cells were centrifuged twice (1 min, 800 *g*) to remove unbound aptamer−gold conjugates. Reflectance imaging of the labeled cells was performed with confocal microscopy (Zeiss LSM510) in reflectance mode (633 nm laser, 63× objective). *Image J* software was used to compare the signal intensity of the reflectance images obtained from the two cell lines.

III. RESULTS AND DISCUSSION

Figure 1 illustrates the steps involved in conjugating anti-PSMA aptamers to gold nanoparticles. Gold nanoparticles are first coated with aptamer capture oligonucleotides via the gold−sulfur interactions between the lattice structure of the gold nanoparticles and the thiol groups of the aptamer capture oligonucleotide. Due to the strong gold−sulfur binding energy (*11*), most conjugation approaches to gold nanoparticles are based on this interaction. A PEG spacer is added between the thiol and the complementary capture sequence of the oligonucleotide to improve hybridization efficiency by minimizing steric hindrance between the gold surface and the hybridization site. The use of oligonucleotide coating on gold nanoparticles has several advantages. First, the negatively charged phosphate groups present on the oligonucleotides prevent aggregation of the nanoparticles via electrostatic repulsion. This results in stable gold nanoparticles that do not aggregate even in high salt environments (i.e., physiological buffers). Second, the presence of the capture oligonucleotides on the gold nanoparticles can be used to easily conjugate other targeting moieties which incorporate a complementary sequence. In this study, an extended anti-PSMA aptamer is then hybridized to the aptamer-capture oligonucleotides on the gold nanoparticles. A major advantage of this conjugation approach is that it prevents any direct modification of the aptamer sequence involved in the binding process, since conjugation to gold nanoparticles is facilitated via the oligonucleotide extension. A longer spacer composed of PEG, polyA's, or polyT's can also be used if larger gold nanoparticles (40−100 nm diameter) are desired. Larger

Table 1. Characterization of Aptamer−Gold Conjugates

	hydrodynamic size (diameter), nm	number of oilgonucleotide per Au nanoparticle
bare Au nanoparticle	19.3 ± 0.6	N/A
Au nanoparticle + aptamer capture oilgonucleotide	25.5 ± 1.2	376 ± 25 (aptamer capture)
Au nanoparticle + aptamer capture oilgonucleotide + anti-PSMA aptamer	39.6 ± 3.8	213 ± 12 (anti-PSMA aptamer)

nanoparticles can provide higher contrast images but can present difficulties during delivery and clearance routes.

Table 1 summarizes the characteristics of the gold nanoparticle conjugates used in this study. The bare gold nanoparticles were measured to have an average hydrodynamic diameter of 19.3 nm. The addition of the aptamer-capture oligonucleotide resulted in nanoparticles with an average diameter of 25.5 nm, an increase of 6.2 nm. This is consistent with the expected size contribution of the added aptamer-capture oligonucleotide (24 nucleotides + hexa(ethylene glycol) spacer) of about ~3 nm on each side based on the predicted hairpin structure. Upon hybridization of the anti-PSMA aptamers, the average nanoparticle size was 39.6 nm, an increase of 20.3 nm compared to the bare gold nanoparticles. Again, the expected size contribution of the added extended A9 anti-PSMA aptamer (94 nucleotides) is between 8 and 10 nm on each side based on the predicted m-fold RNA secondary structure. In summary, the measured sizes of the functionalized gold conjugates are within the expected size contribution of the added oligonucleotides. Determining the size of the gold conjugates is an important consideration in the delivery and clearance of the contrast agents for imaging applications.

We also determined the average number of oligonucleotides (both aptamer capture and anti-PSMA aptamers) present per gold nanoparticle (Table 1). Based on measurements using the oligonucleotide quantitation assay, there are approximately 376 aptamer-capture oligonucleotides per gold nanoparticle. This number represents the possible number of hybridization sites for the anti-PSMA aptamers and is consistent with literature values for oligonucleotide coating on various sizes of Au nanoparticles (*12*). Using a fluorescently labeled anti-PSMA aptamer analogue, we determined that there are approximately 213 anti-PSMA aptamer analogues per gold nanoparticle. This represents a 57% conjugation efficiency which can be attributed to the steric hindrance upon hybridization between the aptamer capture oligonucleotide and the anti-PSMA aptamer analogue. The efficiency may be further reduced when using larger oligonucleotides like the extended A9 anti-PSMA aptamer. We did not determine this efficiency directly because of difficulties in modifying the aptamer with fluorescent dyes. Direct quantitation of the aptamer conjugated to gold nanoparticles using oligonucleotide assays is difficult because of the contribution of the aptamer capture oligonucleotide. However, we validated the incorporation of the extended A9 anti-PSMA aptamers on the gold nanoparticles using reflectance imaging. Ideally, only a few copies of the aptamers per gold nanoparticles are necessary to develop a molecular-specific contrast agent for reflectance imaging.

Figure 2 shows the brightfield and reflectance confocal images of PSMA negative (PC3) and PSMA positive (LNCaP) cells labeled with anti-PSMA aptamer−gold conjugates. The reflectance images of the LNCaP positive cell lines show strong labeling with the aptamer−gold conjugates. Minimal labeling was observed for the PC3 negative cell lines. The labeling on the LNCaP positive cells occurs around the cellular membrane, consistent with the expected pattern, since the PSMA target is a membrane-bound glycoprotein. The reflectance images also

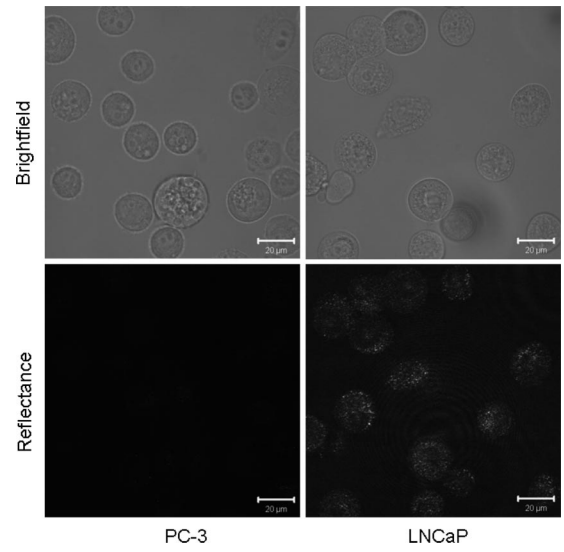

Figure 2. Reflectance imaging using aptamer−gold conjugates. Scale bar is 20 μm.

suggest possible endocytosis of the aptamer−gold conjugates during the labeling process. Analysis of signal intensity using *Image J* software shows a 3−5-fold increase in the reflectance intensity of the positive cell lines compared to intensity of the negative cell lines. For imaging applications, an increase of 1.5- to 3.0-fold in contrast intensity is considered significant (*13*).

There are other important considerations in the use of aptamer−gold conjugates as molecular-specific contrast agents for clinical imaging. For example, the cytotoxicity of the contrast agents should be carefully evaluated. In a previous paper, we evaluated the cytotoxicity of the oligonucleotide-coated gold nanoparticles using standard cell viability assays (*14*). Delivery and clearance routes of the contrast agents are also important factors. We are currently exploring these areas in order to facilitate translation of this type of contrast agents for molecular imaging applications.

IV. CONCLUSION

The study illustrates the feasibility of using aptamer−gold nanoparticles as molecular-specific contrast agents for reflectance imaging. We introduced a new method for conjugating aptamers via hybridization reactions on oligonucleotide-coated gold nanoparticles. An alternative approach for introducing aptamers to gold nanoparticles is the direct use of thiolated aptamers, which has recently been reported (*15*). However, the approach presented in this study has several advantages over the use of thiolated aptamers. First, the integrity and stability of the aptamers is easily preserved during the bioconjugation process since the aptamers are only introduced for a short period of time during the hybridization process. Second, a smaller amount of aptamers can be used for binding to gold nanoparticles, in contrast to thiolated aptamers where significant amounts of aptamers are necessary to coat and stabilize the gold nanoparticles. In our approach, the use of shorter and cheaper complementary oligonucleotides facilitates better coating and stabilization of the gold nanoparticles prior to bioconjugation of the aptamers. Last, our approach offers possible multiplexing capabilities where other types of molecules (targeting, delivery, imaging, or therapeutic) can be incorporated in the design of the contrast agents. In a previous study, we have demonstrated a multimodal reporting system (reflectance and fluorescence) using oligonucleotide−dye conjugates hybridized on complementary oligonucleotides functionalized on gold nanoparticles (*14*). Moreover, therapeutic molecules can be incorporated to

the aptamer-gold nanoparticles to develop multimodal theranostic agents. For example, protein-based therapeutic agents (*16*) can be functionalized via oligonucleotide−protein linkage to aptamer−gold conjugates with the advantage of controlling the amount of therapeutic agents per nanoparticle. The ability to incorporate multifunctional agents into a single construct can be a useful technique in developing multimodal platforms for various clinical applications.

ACKNOWLEDGMENT

We would like to acknowledge Vivian Mack for preparing the cell cultures and BRP R01CA103830 NCI and Center for Biological and Environmental Nanotechnology (CBEN) for funding. Nitin Nitin contributed equally to this manuscript.

LITERATURE CITED

(1) Bunka, D. H., and Stockley, P. G. (2006) Aptamers come of age - at last. *Nat. Rev. Microbiol. 4*, 588–96.

(2) Brody, E. N., and Gold, L. (2000) Aptamers as therapeutic and diagnostic agents. *J. Biotechnol. 74*, 5–13.

(3) Aaron, J., Nitin, N., Travis, K., Kumar, S., Collier, T., Park, S. Y., Jose-Yacaman, M., Coghlan, L., Follen, M., Richards-Kortum, R., and Sokolov, K. (2007) Plasmon resonance coupling of metal nanoparticles for molecular imaging of carcinogenesis in vivo. *J. Biomed. Opt. 12*, 034007. /1−034007/11.

(4) Nitin, N., Javier, D. J., Roblyer, D. M., and Richards-Kortum, R. (2007) Widefield and high-resolution reflectance imaging of gold and silver nanospheres. *J. Biomed. Opt. 12*, 051505. /1−051505/10.

(5) Sokolov, K., Follen, M., Aaron, J., Pavlova, I., Malpica, A., Lotan, R., and Richards-Kortum, R. (2003) Real-time vital optical imaging of precancer using anti-epidermal growth factor receptor antibodies conjugated to gold nanoparticles. *Cancer Res. 63*, 1999–2004.

(6) Aslan, K., Lakowicz, J. R., and Geddes, C. D. (2004) Nanogold-plasmon-resonance-based glucose sensing. *Anal. Biochem. 330*, 145–55.

(7) Aslan, K., Zhang, J., Lakowicz, J. R., and Geddes, C. D. (2004) Saccharide sensing using gold and silver nanoparticles−a review. *J. Fluoresc. 14*, 391–400.

(8) Chu, T. C., Shieh, F., Lavery, L. A., Levy, M., Richards-Kortum, R., Korgel, B. A., and Ellington, A. D. (2006) Labeling tumor cells with fluorescent nanocrystal-aptamer bioconjugates. *Biosens. Bioelectron. 21*, 1859–66.

(9) Lupold, S. E., Hicke, B. J., Lin, Y., and Coffey, D. S. (2002) Identification and characterization of nuclease-stabilized RNA molecules that bind human prostate cancer cells via the prostate-specific membrane antigen. *Cancer Res. 62*, 4029–33.

(10) Mirkin, C. A., Letsinger, R. L., Mucic, R. C., and Storhoff, J. J. (1996) A DNA-based method for rationally assembling nanoparticles into macroscopic materials. *Nature 382*, 607–9.

(11) Rodriguez, J. A., Dvorak, J., Jirsak, T., Liu, G., Hrbek, J., Aray, Y., and Gonzalez, C. (2003) Coverage effects and the nature of the metal-sulfur bond in S/Au(111): high-resolution photoemission and density-functional studies. *J. Am. Chem. Soc. 125*, 276–85.

(12) Hurst, S. J., Lytton-Jean, A. K., and Mirkin, C. A. (2006) Maximizing DNA loading on a range of gold nanoparticle sizes. *Anal. Chem. 78*, 8313–8.

(13) Adams, K. E., Ke, S., Kwon, S., Liang, F., Fan, Z., Lu, Y., Hirschi, K., Mawad, M. E., Barry, M. A., and Sevick-Muraca, E. (2007) Comparison of visible and near-infrared wavelength-excitable fluorescent dyes for molecular imaging of cancer. *J. Biomed. Opt. 12*, 024017. /1−024017/9.

(14) Nitin, N., Javier, D. J., and Richards-Kortum, R. (2007) Oligonucleotide-coated metallic nanoparticles as a flexible platform for molecular imaging agents. *Bioconjugate Chem. 18*, 2090–6.

(15) Medley, C. D., Smith, J. E., Tang, Z., Wu, Y., Bamrungsap, S., and Tan, W. (2008) Gold nanoparticle-based colorimetric assay for the direct detection of cancerous cells. *Anal. Chem. 80*, 1067–1072.

(16) Chu, T. C., Marks, J. W., III, Lavery, L. A., Faulkner, S., Rosenblum, M. G., Ellington, A. D., and Levy, M. (2006) Aptamer:toxin conjugates that specifically target prostate tumor cells. *Cancer Res. 66*, 5989–92.

BC8001248